doi.org/10.36721/PJPS.2023.36.1.SP.345-352.1

Physicochemical characterization and preliminary *in vitro* antioxidant activities of curcumin and meloxicam co-encapsulated PLGA nanoparticles

Bilal Aslam[1]*, Asif Hussain[1], Muhammad Naeem Faisal[1], Muhammad Usman Bari[1], Shaneel Kousar[1,2], Aqsa Mushtaq[1,3], and Asher Umer[1]

[1]Institute of Physiology and Pharmacology, University of Agriculture, Faisalabad, Pakistan
[2]Faculty of Pharmacy, University of Lahore, Lahore, Pakistan
[3]Dow College of Pharmacy, Dow University of Health Sciences, Karachi, Pakistan

Abstract: Nanoformulations (NFs) are suitable for encapsulation and delivery of multiple hydrophobic drugs. Polymers enable higher drug entrapment and sustained drug release profile. In this study, poly(lactic-co-glycolic) acid (PLGA) nanoparticles (NPs) co-encapsulating hydrophobic agents including curcumin (Cur) and meloxicam (Mlx) were prepared and physicochemically characterized. Mono and dual drug loaded NPs of Cur and Mlx were synthesized using single-emulsion (o/w) solvent evaporation method. NPs were characterized for zeta size and potential, polydispersity index (PDI), encapsulation efficiency, *in vitro* drug release and storage stability. *In vitro* antioxidant activity was determined using DPPH and ABTS scavenging assays. Spherical smooth surfaced mono and dual drug-loaded NPs showed particle sizes of 104.2 to 195.4 nm, zeta potential of -22.9 to -17.1 mV and PDI below 0.25. High encapsulation efficiency (>75%) of all drug-loaded NPs was found. NPs exhibited an initial burst following sustained drug release rates at pH 7.4. *In vitro*, Cur and Mlx co-loaded NPs exhibited higher radical scavenging activity compared to pure drugs in DPPH and ABTS assays. Storage stability studies showed insignificant changes in NPs at 4°C and 27°C for one month. Conclusively, Cur and Mlx co-encapsulation resulted in stable NFs with high drug encapsulation efficiencies, improved drug release profiles and antioxidant activities.

Keywords: Antioxidant, co-encapsulation, curcumin, meloxicam, nanoparticles, PLGA.

INTRODUCTION

Nanoformulations (NFs), as targeted drug delivery systems, have gained more attention from researchers in the last few decades. Nanoparticles (NPs) are formulated as colloidal systems with particle sizes ranging from 10 nm to 1000 nm. Biodegradable polymers are used to adsorb, entrap or chemically couple the active substances (Li *et al*., 2022). In contrast to conventional drug delivery systems, NPs have several advantages such as enhanced stability, hydrophobic and hydrophilic drug incorporation, administration through different routes, reduction in administration frequency and fewer side effects. Drugs having poor absorption can be incorporated into NPs to enhance their bioavailability, controlled release and prolong the drug residence time in the body (Saxena *et al*., 2020).

Polymers include poly (D, L-lactic-co-glycolic) acid (PLGA) is widely used to prepare controlled release NPs for human use due to its non-immunogenic, biocompatible and biodegradable features (Rocha *et al*., 2022). Lactic acid and glycolic acid are two monomeric parts of PLGA that are obtained upon polymer hydrolysis. Being endogenous compounds lactic acid and glycolic acid are readily metabolized in the body. Therefore, PLGA NPs are associated with minimal systemic toxicities (Ghitman *et al*., 2020). Stabilizing agents are used to reduce the interfacial tension between hydrophobic and hydrophilic phases consequently stabilizing the colloidal dispersion. Polyvinyl alcohol (PVA) or other types of pluronics are used to incorporate hydrophobic substances into NPs (Arefian *et al*., 2020).

It is well established that excessive production of reactive oxygen species (ROS) plays a crucial role in the pathogenesis of various chronic inflammatory diseases. In recent years research focus is increased to employ antioxidant therapies in the management of oxidative stress-mediated pathological abnormalities (Zhong *et al*., 2021). Curcumin (Cur), a polyphenol extracted from the rhizome of *Curcuma longa*, is well studied for its potential antioxidant, anti-inflammatory, anti-microbial and anti-carcinogenic activities. Studies have shown the effectiveness of Cur in the treatment of rheumatoid arthritis, Alzheimer's disease, multiple sclerosis and atherosclerosis (Salehi *et al*., 2019; Guan and Gao, 2022). Also, Cur inhibits metastasis, cell proliferation and induces apoptosis mediated by growth factors and pro-inflammatory factors (Kabir *et al.,* 2021). However, the poor aqueous solubility of Cur limits its widespread clinical applications. Several researchers have attempted to develop Cur encapsulated NFs to evade the low solubility problem (Lu *et al.*, 2020; Wu, 2021).

**Corresponding author:* e-mail: bilal.aslam@uaf.edu.pk

Meloxicam (Mlx) belongs to the non-steroidal anti-inflammatory drugs (NSAIDs). It prevents the production of pro-inflammatory prostaglandins (PGs) by selectively inhibiting cyclooxygenase-2 (COX-2). In addition, the antioxidant potential of Mlx is reported to strengthen the antioxidant defense system and inhibit cell apoptosis, ameliorate liver toxicity and is believed to be responsible for its neuroprotective action (Pawlukianiec *et al.,* 2020). The combination of Mlx with other natural/synthetic agents has shown synergistic pharmacological activities in various pathological conditions (Gutierrez *et al*., 2021; Wasay *et al*., 2022).

Co-encapsulation of multiple therapeutic compounds within a single nano-delivery system has attained significant attention in recent years. Multiple drugs co-loaded nano-carriers can act synergistically with better target selectivity, therapeutic efficacy and low toxicity (Liu *et al*., 2022). Therefore, this study aimed to synthesize, characterize and explore the *in vitro* antioxidant activities of Cur and Mlx co-encapsulated PLGA NPs.

MATERIALS AND METHODS

Drugs and chemicals

Curcumin (Spectrum®, China), meloxicam (Sigma-Aldrich®, USA), poly(lactic-co-glycolic) acid (PLGA) of MW 7,000-17,000 (Sigma-Aldrich®, USA) and polyvinyl alcohol (PVA) 1500 (Duksan® Pure Chemicals, Korea) were procured.

Preparation of NPs

A modified method of Mora-Huertas, (2010) was adopted to prepare Cur, Mlx and Cur plus Mlx loaded NPs *via* a single-emulsion (o/w) solvent evaporation method. Organic phase contained PLGA polymer dissolved in acetone (200mg/mL) and aqueous phase consisted of PVA (2%, w/v) solution. Accurately weighed 10mg of Cur and Mlx alone and in three combinations (ratio 25:75, 50:50 and 75:25) were separately dissolved in 1.5mL of acetone-dichloromethane (1:2, v/v) solvent mixture. PLGA solution and drugs dissolved solvent mixture were emulsified with 10 mL of PVA solution using a micro-tip probe sonicator (Sonics & Materials, Inc., USA) for 30 seconds at 50W output in an ice bath. Then, the formulations were continuously stirred to completely evaporate the organic phase at 37°C using a magnetic stirrer, leaving behind the colloidal suspension of blank NPs (NP-B), Cur loaded NPs (NP-C), Mlx loaded NPs (NP-M) and different combinations of Cur plus Mlx co-encapsulated NPs i.e. NP-CM1 (25:75), NP-CM2 (50:50) and NP-CM3 (75:25). NFs were centrifuged at 25000 rpm for 10 minutes and NPs in pellet form and the supernatants were collected for further analysis.

Particle size, zeta potential and polydispersity index (PDI)

All NPs were subjected to particle size, zeta potential and PDI characterization (Siddique *et al*., 2021). The collected pellets re-suspended in deionized water and sonicated for 30 seconds were analyzed using Zeta Sizer 3000 (Malvern®, UK).

Encapsulation efficiency (%)

The encapsulation efficiency of NPs was determined by pelletizing the samples at 25,000 rpm for 20 minutes under a controlled temperature (4°C). Then, supernatants were collected and absorbance (λ_{max}: 427 nm for Cur, 363 nm for Mlx) was measured using a spectrophotometer (Shimadzu®, Japan). Different concentrations of Cur and Mlx were used to prepare the calibration curve and encapsulation efficiency was calculated by using an indirect method of Sun *et al*., (2015) as Encapsulation efficiency (%) = [(Encapsulated drug - Free drug)/ Total added drug] x 100.

Fourier transform infrared spectroscopy (FT-IR)

The FT-IR analysis was performed to observe the extent of bonding and drug-polymer interactions between entrapped drugs and polymer. Each lyophilized NPs sample (5 mg) compressed (1000 psi) in 100 mg of KBr was analyzed using FT-IR spectroscope (Spectrum Two®, Perkin Elmer) connected with Spectrum® 10.5.3 software. Absorption spectra of samples were measured from 4000 to 600 cm^{-1} in the IR region (Hussain *et al*., 2021).

Table 1: Particle size, zeta potential and PDI of Cur and Mlx mono and dual drug encapsulated NPs.

Sample	Particle size (nm)	Zeta potential (mV)	PDI
NP-B	10.3	-24.4	0.07
NP-C	138.8	-20.8	0.19
NP-M	104.2	-21.7	0.18
NP-CM1	190.1	-22.9	0.24
NP-CM2	195.4	-17.1	0.21
NP-CM3	171.9	-20.2	0.22

Table 2: Encapsulation efficiency of Cur and Mlx encapsulated NPs.

Sample	Cur content (%)	Mlx content (%)
NP-B	---	---
NP-C	93.16	---
NP-M	---	89.71
NP-CM1	88.90	86.36
NP-CM2	91.84	90.23
NP-CM3	88.42	77.31

Thermo-gravimetric (TGA-DSC) analysis

The thermo-gravimetric analysis of NPs was carried out to observe possible drug-polymer interactions using TA

Instrument Q600 DSC (New Castle, Delaware, USA). Each sample (3-5 mg) was transferred into aluminum crucibles and heated from room temperature to 300°C maintaining the heating rate at 10°C/minute and nitrogen gas flow rate at 100mL/minute.

Scanning electron microscopy (SEM)
Surface morphology of NPs was visualized by SEM (JSM5910, Jeol, Japan). One drop of a concentrated aqueous suspension of NPs was placed and allowed to dry on a metal grid for 24 hours at room temperature. Samples were coated with gold-palladium and analyzed under an argon atmosphere (Kızılbey, 2019).

Storage stability study
Equal quantities (5 mg) of NPs re-suspended in deionized water were separately stored for one month at 4°C and 27°C. Samples were assayed after a pre-estimated time to observe the changes in particle size, zeta potential and PDI (Wan *et al*., 2018).

In vitro release study
Drug release profile of NPs was determined using USP apparatus 2 (Paddle apparatus) according to Sun *et al*., (2015). Egg membrane used as a dialysis membrane was soaked overnight in PBS (pH 7.4) before conducting the analysis. The purified NPs equivalent to 10 mg drug was placed in a dialysis membrane, tied with heat resistant thread and dipped in 500mL of PBS (pH 7.4) with continuous agitation. About 10mL of PBS was withdrawn at specific intervals (0.2, 0.4, 1, 2, 3, 5, 8, 12 and 24 hours) and an equal volume of PBS was substituted to maintain the sinking conditions. Absorbance was measured at 363nm and 427nm using a spectrophotometer (Shimadzu®, Japan) and cumulative percentage release was calculated. All measurements were taken in triplicate.

DPPH radical scavenging assay
The DPPH* scavenging photometric assay with some modification was performed to assess the antioxidant activity of NPs (Subhan *et al*., 2021). Test samples include pure Cur and Mlx and mono and dual drug loaded NPs diluted in ethanol (1000µg/mL) were added to 2 mL of ethanolic DPPH (200µg/mL) to prepare different concentrations (100 to 6.25µg/mL). Samples were incubated at 25°C for 30 minutes and absorbance was taken at 517 nm. The percentage inhibition of DPPH* was calculated by the given formula: DPPH* inhibition (%) = [(A-Control – A-Sample)/A-Control] x 100. A-Control is absorbance of DPPH without sample and A-Sample is absorbance of DPPH with the sample.

ABTS radical scavenging assay
Radical scavenging activity of NPs was determined using ABTS radical decolorization assay (More and Makola, 2020). The production of ABTS cation radical was accomplished by mixing ABTS (10 mg) and potassium persulfate (2 mg) in deionized water and storing in dark for 18-20 hours. Then, ABTS solution (500µL) was diluted with 30mL of methanol. Different concentrations (100-6.25µg/mL) of each NPs and pure drugs were prepared and added to ABTS methanolic solution. Absorbance was measured at 734 nm after incubating the test samples for 30 minutes at room temperature. The percentage inhibition (%) of ABTS was calculated using the above-mentioned formula.

STATISTICAL ANALYSIS

Results obtained from *in vitro* antioxidant assays were analyzed by applying two-way ANOVA and Tukey's test using GraphPad Prism® software (version 6.01), considering $P<0.05$ as a significant difference. Triplicate values were presented as Mean±SD.

RESULTS

Particle size, zeta potential and PDI of NPs
As mentioned in table 1, Cur and Mlx mono and dual drug loaded NPs showed particle sizes ranging from 104.2 nm to 195.4 nm along with PDI values less than 0.25. Zeta potential values were recorded from -22.9 mV to -17.1 mV.

Encapsulation efficiency of NPs
The encapsulation efficiency of prepared NPs was determined by the indirect method. NPs encapsulate Cur and Mlx alone and in different combinations showed encapsulation efficiency of more than 75% (table 2).

FT-IR analysis of NPs
The FT-IR spectra of PLGA, Cur and Mlx standards are shown in fig.1 (A-C). The spectra for drug loaded NPs (fig. 1D-F) revealed similarity to the PLGA spectrum. The obtained results showed the peak at ~1729 cm^{-1} indicate the C=O ester bond stretching of PLGA. Peaks in the region of 1100-1400 cm^{-1} are representing C-O stretches for the samples. PLGA and co-encapsulated NPs showed a peak at ~2929 cm^{-1} which indicate C-H bond stretching. The characteristic peaks of Cur and Mlx at ~1580 cm^{-1} and ~3290 cm^{-1} represent stretching of C=N and O-H bonds, respectively were also noticed for dual drug loaded NPs.

Thermo-gravimetric analysis of NPs
The thermo-gravimetric behavior of pure PLGA, Cur, Mlx and dual drug loaded NPs was assessed using TGA-DSC analysis as shown in fig. 2(A-F). Thermograms of PLGA, Cur and Mlx demonstrated two thermal peaks; an initial phase transition peak at 53.6°C, 182.7°C and 223.4°C and a second peak at 228.1°C, 224.9°C and 265.2°C, respectively indicating thermal degradation of pure compounds (fig. 2A-C). However, dual drug loaded NPs encapsulating Cur and Mlx (fig. 2D-F) showed a single broadened peak at 229.6°C, 226.9°C and 232.3°C, respectively.

Table 3: Particle size, zeta potential and PDI of Cur and Mlx mono and dual drug encapsulated NPs after one month (4°C and 27°C).

Sample	Particle size (nm)		Zeta potential (mV)		PDI	
	4°C	27°C	4°C	27°C	4°C	27°C
NP-B	24.3	18.1	-19.9	-22.6	0.17	0.11
NP-C	190.1	159.2	-13.2	-17.3	0.29	0.24
NP-M	147.6	122.4	-14.8	-19.1	0.30	0.21
NP-CM1	244.8	220.1	-16.1	-20.8	0.32	027
NP-CM2	278.0	241.7	-14.9	-18.3	0.22	0.19
NP-CM3	236.2	199.9	-11.5	-15.1	0.33	0.26

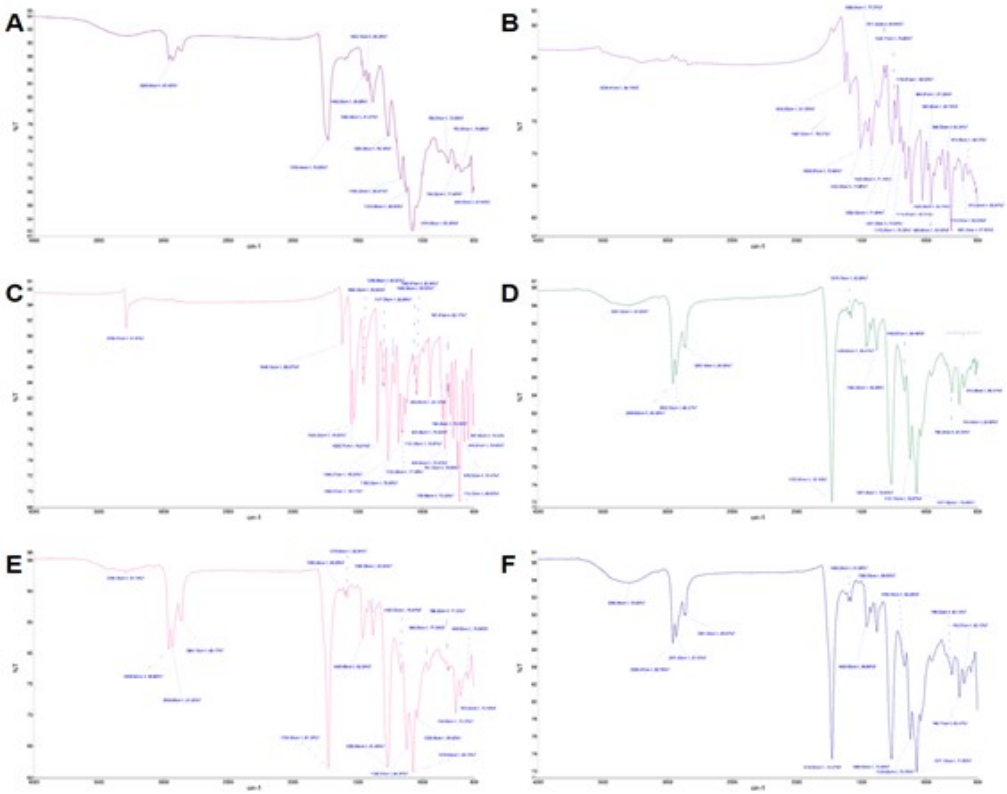

Fig. 1: FT-IR spectra of standards (A) PLGA, (B) Cur and (C) Mlx and dual drug loaded NPs (D) NP-CM1, (E) NP-CM2 and (F) NP-CM3, respectively.

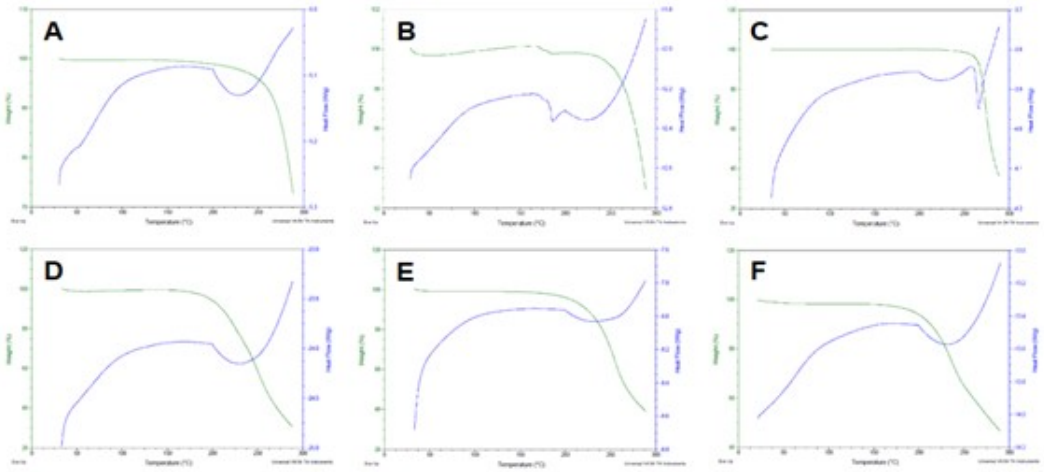

Fig. 2: Thermograms of standards (A) PLGA, (B) Cur and (C) Mlx and dual drug loaded NPs (D) NP-CM1, (E) NP-CM2 and (F) NP-CM3, respectively.

SEM analysis of NPs

Surface morphological features of PLGA-based NPs were observed under SEM. NPs loaded with mono and dual drugs showed nearly spherical and smooth surfaces without any significant adhesion or aggregation (fig. 3A-E). In addition, some NPs with a porous surface were also found.

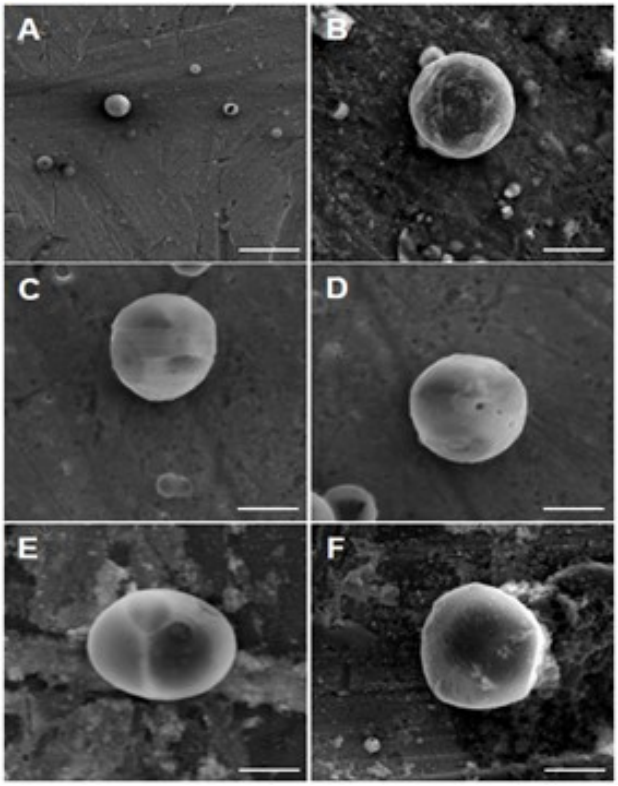

Fig. 3: SEM microphotographs showing smooth-surfaced spherical NPs. (A) NP-B, (B) NP-C, (C) NP-M, (D) NP-CM1, (E) NP-CM2 and (F) NP-CM3.

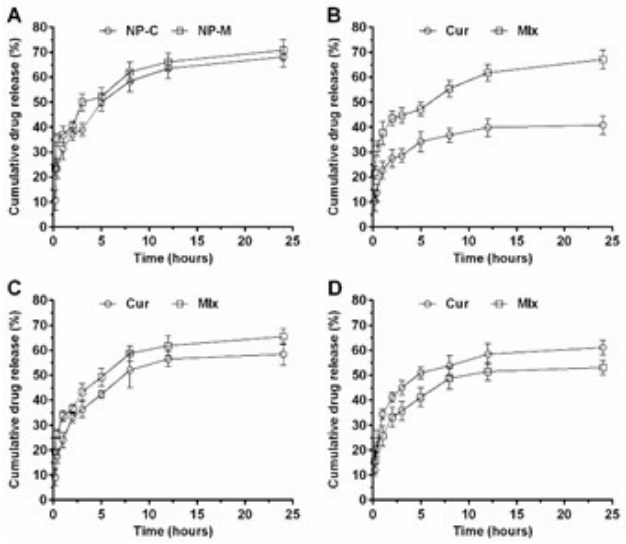

Fig. 4: *In vitro* drug release profile of mono drug loaded NP (A) NP-C and NP-M and dual-drug loaded NP (B) NP-CM1, (C) NP-CM2 and (D) NP-CM3. Results are presented as Mean±SD (n=3).

Storage stability studies of NPs

To assess the storage stability, Mlx and Cur loaded NPs were stored at 4°C and 27°C for one month. After the predetermined time, samples of each NPs were evaluated for the changes in zeta size, zeta potential and PDI. Results presented in table 3 indicate insignificant changes in particle size, zeta potential and PDI of all NPs at 27°C compared to that stored at 4°C.

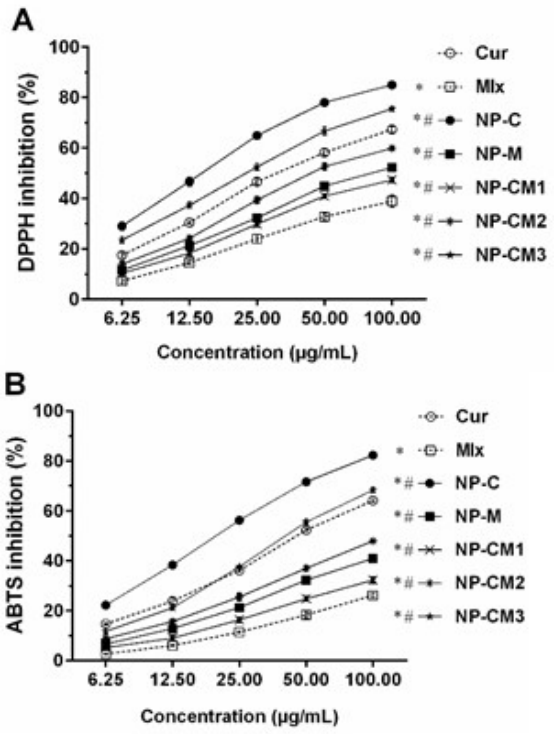

Fig. 5: *In vitro* antioxidant activity of pure Cur and Mlx and NPs loaded with Cur and Mlx mono and dual drug loaded NPs in (A) DPPH* scavenging assay and (B) ABTS* scavenging assay. Results are presented as Mean±SD (n=3). *P<0.05 significant difference from pure Cur; #P<0.05 significant difference from pure Mlx.

In vitro drug release of NPs

Results presented in fig. 4(A-D) showed the drug release profile of Cur and Mlx encapsulated NPs in a dissolution medium (pH 7.4) for 24 hours. All NPs exhibited a biphasic drug release pattern for 24 hours. An initial burst release of Cur or/and Mlx was seen from NPs for 5 hours and then sustained drug release was observed up to 24 hours. Results demonstrated that 68.11±4.12% and 70.78±4.23% of Cur and Mlx, respectively were released from mono drug loaded NPs in 24 hours (fig. 4A). Three combinations of co-drug loaded NPs showed 42.12±2.10%, 58.44±2.52% and 61.84±1.64% of Cur release and cumulative release of Mlx was 67.11±2.20%, 65.90±1.81% and 53.46±1.25%, respectively (fig. 4B-D).

In vitro antioxidant activity of NPs

The radical scavenging activity of different concentrations, ranging from 6.25-100 µg/mL, of mono

and dual drug loaded NPs in comparison to pure Cur and Mlx was assessed using DPPH and ABTS assays as mentioned in fig. 5 (A, B). In both tests, the test samples demonstrated free radical scavenging activity in a dose-dependent manner. The NP-C and NP-M showed a significantly increased DPPH scavenging activity from 28.99±1.62% to 84.01±1.25% and 11.55±0.81% to 52.24±0.98% in comparison to pure Cur (17.34±0.95% to 67.43±1.32%) and Mlx (7.26±1.03% to 38.57±2.31%). The free radical scavenging activity of dual drug loaded NPs i.e. NP-CM1, NP-CM2 and NP-CM3 was found in the range of 10.82±0.84% to 47.62±0.63%, 13.19±0.59% to 59.91±0.82%, and 23.51±1.71% to 75.53±0.85%, respectively (fig. 5A). Similarly, ABTS radical scavenging ability of mono- and dual-drug loaded NPs were observed in the range of 22.28±0.96% to 82.27±1.04% for NP-C, 6.63±0.94% to 40.97±1.28% for NP-M, 5.19±0.91% to 32.28±1.04% for NP-CM1, 8.79±0.85% to 47.97±1.18% for NP-CM2 and 11.70±1.28% to 68.36±1.10% for NP-CM3, respectively as compared to pure Cur (14.67±0.49% to 64.19±0.67%) and Mlx (2.67±0.51% to 26.21±0.95%) (fig. 5B).

DISCUSSION

Oxidative stress is believed to be associated with the onset and persistence of various autoimmune and chronic inflammatory diseases. Therefore, anti-inflammatory agents along with antioxidants are becoming suitable approaches for the prevention and treatment of inflammatory conditions (Ijaz *et al*., 2021). Cur is a well-known natural compound famous for its antioxidant and anti-inflammatory activities (Salehi *et al*., 2019). Mlx a potent synthetic NSAID, is efficient in relieving inflammation and pain. Mlx is preferred over other NSAIDs due to its low toxicity and appreciable tolerability (Pawlukianiec *et al.,* 2020). However, poor aqueous solubility and low bioavailability are some limitations of the use of Cur and Mlx. NFs are being used as a single or/and co-drug delivery system to overcome the aforementioned drawbacks of hydrophobic drugs and to improve the therapeutic efficacy and targeted drug delivery of conventional drugs (Liu *et al*., 2022). Here, dual drug loaded PLGA NPs encapsulating Cur and Mlx were successfully prepared and characterized.

Optimization of NPs to adjust the particle size of dual drug loaded NPs appears to be based on similar principles as single-agent loaded NPs prepared by the single emulsion (o/w) evaporation method. The emulsification process and stability of emulsion globules are the main controlling factors of particle size, while drug entrapment efficiency depends upon the partition of the drug in aqueous-organic phases and drug-polymer interactions. The particle size mainly contributes to the improved bioavailability of drug-loaded NPs (Hernández-Giottonini *et al*., 2020). Deprotonating free carboxylic groups of PLGA leads to a negatively charged polymer chain that imparts negative zeta potential. In comparison to large size NPs, small size NPs tend to have high zeta potential values which result in increased stability of NPs (Kızılbey, 2019; Ovenseri and Halilu, 2022). In the present study, PLGA NPs encapsulating single and three combinations of Cur and Mlx showed particle sizes ranging from 104.2 nm to 195.4 nm, PDI less than 0.25 and zeta potential from -22.9 mV to -17.1 mV, which indicate the good uniformity and colloidal stability of all NPs (table 1).

Encapsulation or entrapment efficiency (%) of NPs can be determined through a direct or indirect method. Free drug present in supernatant after centrifugation of NPs is measured through an indirect method and is used to estimate the encapsulation efficiency (Wan *et al*., 2018). Results revealed the high encapsulation efficiency (>75%) of prepared mono and dual drug loaded NPs determined through an indirect method (table 2).

The FT-IR analysis of standard PLGA, Cur and Mlx and dual drug loaded NPs was carried out to highlight any drug-polymer interactions (fig. 1A-F). The presence of characteristic peaks of PLGA at ~1729 cm^{-1} (C=O stretching), ~2929 cm^{-1} (C-H stretching) and 1100-1400 cm^{-1} (C-O stretching) in the FT-IR spectra of dual drug load NPs indicated the drug-polymer compatibility. In addition, distinctive peaks of standard Cur at ~1580 cm^{-1} (C=N stretching) and Mlx at ~3290cm^{-1} (O-H stretching) were also noticed in dual drug loaded NPs which showed the chemical stability of Cur and Mlx in all NPs as observed in the previous study (Akel *et al*., 2021).

The thermo-gravimetric analysis demonstrates the thermal transition, degradation and stability characteristics of materials as a function of temperature (Wasay *et al*., 2022). Initially, materials show a small mass loss in the first transition step followed by significant mass loss due to the degradation of material (Sun *et al*., 2015). In this study, thermo-gravimetric changes of pure PLGA, Cur and Mlx and NPs encapsulating Cur and Mlx in three combinations were observed (fig. 2A-F). Thermo grams of pure compounds showed two thermal peaks indicating initial phase transition and later degradation of PLGA, Cur and Mlx. While, a single broadened peak of dual drug loaded NPs suggests the insignificant drug-polymer interaction and improved stability and sustained release nature of NPs as observed previously (Arzani *et al*., 2019; Akel *et al*., 2021).

SEM analysis showed the spherical smooth-surfaced NPs with narrow particle size distribution. An insignificant difference was observed in the surface morphology of blank, mono and co-drug loaded NPs (fig. 3A-F). Size distributions obtained from SEM results were nearly similar to that measured from DLS. However, minor

differences in size measurement were found as SEM analysis is performed using dry state NPs while DLS measures the hydrodynamic size of dispersed NPs. Few NPs with porous surfaces were also observed, which is likely to be beneficial for drug dissolution and subsequent degradation of polymer (Khan *et al*., 2020).

The storage stability of NFs is a critical parameter for all pharmaceuticals. Blank, mono and co-encapsulated NPs of Cur and Mlx stored at 4^{o}C and 27^{o}C for one month exhibited minor changes in the size, zeta potential and PDI in both cases (table 3). It indicates the stability of formulated NPs in these particular conditions. Our findings are in concordance with the previous study (Zhang *et al*., 2022).

In vitro drug release study of NPs loaded with hydrophobic drugs (Cur and Mlx) bearing more than 75% encapsulation efficiency was carried out for 24 hours. All NPs showed drug release in a biphasic pattern (fig. 4A-D). The initial phase of abrupt drug release indicated the rapid dissolution of the adsorbed drug on the surface of NPs followed by sustained drug release that could be due to slow penetration of diffusion medium into NPs. Therefore, the rate of drug diffusion through polymer is assumed as the main factor controlling the drug release from NPs as reported in a previous study (Grune *et al*., 2021).

DPPH and ABTS radical scavenging assays were applied to assess the antioxidant activities of Cur and Mlx in free and encapsulated NPs forms. In both assays, PLGA encapsulating Cur and Mlx showed significantly ($P<0.05$) enhanced antioxidant activities when compared to pure drugs (fig. 5A, B). Results indicate that the prepared mono and dual drug loaded NPs have promising antioxidant potential. Moreover, dual drug loaded NPs demonstrated additive antioxidant effects. Hence, co-encapsulation of Cur and Mlx improved the bioavailability as well as may contribute to antioxidant effects in the oxidative stress-mediated pathological conditions as reported in the previous study (Patergnani *et al*., 2021; Widowati *et al*., 2022).

CONCLUSION

The present study demonstrated the successful preparation of Cur and Mlx co-encapsulated PLGA NPs using a single emulsion (o/w) solvent evaporation technique. Our findings also indicated the high drug entrapment efficiency of mono and dual drug loaded NPs with improved sustained release profiles and enhanced antioxidant activities of all formulations. Hence, these NPs have potential to act as nano-carriers for the co-delivery of Cur and Mlx. Thus, our findings suggest that the dual drug loaded NPs may be applied in the clinical setting for the management of inflammatory conditions. Furthermore, we aim to investigate any possible synergistic anti-inflammatory and anti-arthritic activities of prepared dual drug loaded NPs in future studies.

ACKNOWLEDGMENT

This study was fully supported by HEC, Pakistan-funded project (Project ID: 7510/Sindh/NRPU/R&D/HEC/2017).

REFERENCES

Akel H, Ismail R, Katona G, Sabir F, Ambrus R and Csóka I (2021). A comparison study of lipid and polymeric nanoparticles in the nasal delivery of meloxicam: Formulation, characterization and *in vitro* evaluation. *Int. J. Pharm*., **604**(7): e120724.

Arefian M, Hojjati M, Tajzad I, Mokhtarzade A, Mazhar M and Jamavari A (2020). A review of polyvinyl alcohol/carboxymethyl cellulose (PVA/CMC) composites for various applications. *J. Compos. Compd.*, **2**(3): 69-76.

Arzani H, Adabi M, Mosafer J, Dorkoosh F, Khosravani M, Maleki H and Kamali M (2019). Preparation of curcumin-loaded PLGA nanoparticles and investigation of its cytotoxicity effects on human glioblastoma U87MG cells. *Biointerface Res. Appl. Chem*., **9**(5): 4225-4231.

Ghitman J, Biru EI, Stan R and Iovu H (2020). Review of hybrid PLGA nanoparticles: Future of smart drug delivery and theranostics medicine. *Mater. Des*., **193**(8): e108805.

Grune C, Zens C, Czapka A, Scheuer K, Thamm J, Hoeppener S, Jandt KD, Werz O, Neugebauer U and Fischer D (2021). Sustainable preparation of anti-inflammatory atorvastatin PLGA nanoparticles. *Int. J. Pharm*., **599**(4): e120404.

Guan W and Gao H (2022). Potential of curcumin loaded nanoparticles in ovarian cancer: Investigation using gynecological color Doppler ultrasound technique. *Pak. J. Pharm. Sci*., **35**(5): 1467-1471.

Gutierrez MEZ, Savall ASP, da Luz Abreu E, Nakama KA, Dos Santos RB, Guedes MCM and Pinton S (2021). Co-nanoencapsulated meloxicam and curcumin improves cognitive impairment induced by amyloid-beta through modulation of cyclooxygenase-2 in mice. *Neural Regen. Res*., **16**(4): 783-789.

Hernández-Giottonini KY, Rodríguez-Cordova RJ, Gutiérrez-Valenzuela CA, Penunuri-Miranda O, Zavala-Rivera P, Guerrero-Germán P and Lucero-Acuña A (2020). PLGA nanoparticle preparations by emulsification and nanoprecipitation techniques: Effects of formulation parameters. *Rsc Advances*, **10**(8): 4218-4231.

Hussain A, Aslam B, Muhammad F, Faisal MN, Kousar S, Mushtaq A and Bari MU (2021). Anti-arthritic activity of *Ricinus communis* L. and *Withania somnifera* L. extracts in adjuvant-induced arthritic rats

via modulating inflammatory mediators and subsiding oxidative stress. *Iran. J. Basic Med. Sci.*, **24**(7): 951-961.

Ijaz MU, Aziz S, Faheem M, Abbas K, Nasir S, Naz H, Ali A and Imran M (2021). Orientin attenuates cisplatin-induced renal toxicity by reducing oxidative stress and inflammation. *Pak. Vet. J*., **41**(4): 574-578.

Kabir M, Rahman M, Akter R, Behl T, Kaushik D, Mittal V, Pandey P, Akhtar MF, Saleem A, Albadrani GM and Kamel M (2021). Potential role of curcumin and its nanoformulations to treat various types of cancers. *Biomolecules*, **11**(3): e392.

Khan MM, Madni A, Nayab T, Khan FP, Khan S, Jan N, Ali A and Khan MI (2020). Co-delivery of curcumin and cisplatin to enhance cytotoxicity of cisplatin using lipid-chitosan hybrid nanoparticles. *Int. J. Nanomed*., **15**(1): 2207-2217.

Kızılbey K (2019). Optimization of rutin-loaded PLGA nanoparticles synthesized by single-emulsion solvent evaporation method. *Acs Omega*, **4**(1): 555-562.

Li X, Montague EC, Pollinzi A, Lofts A and Hoare T (2022). Design of smart size^{-}, surface^{-} and shape^{-} switching nanoparticles to improve therapeutic efficacy. *Small*, **18**(6): e2104632.

Liu K, Chen YY, Pan LH, Li QM, Luo JP and Zha XQ (2022). Co-encapsulation systems for delivery of bioactive ingredients. *Food Res. Int.*, **155**(5): e111073.

Lu L, Qi S, Chen Y, Luo H, Huang S, Yu X and Zhang Z (2020). Targeted immunomodulation of inflammatory monocytes across the blood-brain barrier by curcumin-loaded nanoparticles delays the progression of experimental autoimmune encephalomyelitis. *Biomaterials*, **245**(7): e119987.

Mora-Huertas CE, Fessi H and Elaissari A (2010). Polymer-based nanocapsules for drug delivery. *Int. J. Pharm*., **385**(1-2): 113-142.

More GK and Makola RT (2020). *In-vitro* analysis of free radical scavenging activities and suppression of LPS-induced ROS production in macrophage cells by *Solanum sisymbriifolium* extracts. *Sci. Rep*., **10**(1): 1-9.

Ovenseri AC and Halilu EM (2022). Formulation *and in vitro* evaluation of polymeric metronidazole nanoparticles. *Pak. J. Pharm. Sci*., **35**(5): 1333-1338.

Patergnani S, Bouhamida E, Leo S, Pinton P and Rimessi A (2021). Mitochondrial oxidative stress and Mito-Inflammation: Actors in the diseases. *Biomedicines*, **9**(2): e216.

Pawlukianiec C, Gryciuk ME, Mil KM, Zendzian-Piotrowska M, Zalewska A and Maciejczyk M (2020). A new insight into meloxicam: Assessment of antioxidant and anti-glycating activity *in vitro* studies. *Pharmaceuticals*, **13**(9): e240.

Rocha CV, Gonçalves V, da Silva MC, Bañobre-López M and Gallo J (2022). PLGA-Based composites for various biomedical applications. *Int. J. Mol. Sci*., **23**(4): e2034.

Salehi B, Stojanovic-Radic Z, Matejic J, Sharifi-Rad M, Kumar NVA, Martins N and Sharifi-Rad J (2019). The therapeutic potential of curcumin: A review of clinical trials. *Eur. J. Med. Chem*., **163**(12): 527-545.

Saxena SK, Nyodu R, Kumar S and Maurya VK (2020). Current advances in nanotechnology and medicine. *Nano Bio Medicine*, pp.3-16.

Siddique R, Muhammad F, Aslam B and Faisal MN (2021). Characterization and *in vivo* evaluation of nano formulations in FCA induced rheumatoid arthritis in rats. *Pak. J. Pharm. Sci.,* **34**(2 Suppl.): 787-793.

Subhan F, Aslam B, Muhammad F, Faisal MN, Hussain A and Bari MU (2021). The efficiency of *Cressa cretica* (Linn.) extract in attenuating vancomycin-induced nephrotoxicity and oxidative stress in rabbits. *Comp. Clin. Path*., **30**(8): 829-839.

Sun SB, Liu P, Shao FM and Miao QL (2015). Formulation and evaluation of PLGA nanoparticles loaded capecitabine for prostate cancer. *Int. J. Clin. Exp. Med*., **8**(10): 19670-19681.

Wan S, Zhang L, Quan Y and Wei K (2018). Resveratrol-loaded PLGA nanoparticles: Enhanced stability, solubility and bioactivity of resveratrol for non-alcoholic fatty liver disease therapy. *R. Soc. Open Sci*., **5**(11): e181457.

Wasay SA, Jan SU, Akhtar M, Ahmad R, Shah PA, Razaque G, Muhammad S, Shahwani NA, Younis M, Shahwani GM and Achakzai JK (2022). Meloxicam loaded hydroxypropyl methylcellulose (HPMC) microparticulate: Fabrication, characterization and *in vivo* pharmacokinetic assessment. *Pak. J. Pharm. Sci.*, **35**(4): 1251-1260.

Widowati W, Prahastuti S, Hidayat M, Hasiana ST, Wahyudianingsih R, Afifah E, Kusuma HS, Rizal R and Subangkit M (2022). Protective effect of ethanolic extract of Jati Belanda (*Guazuma ulmifolia* L.) by inhibiting oxidative stress and inflammatory processes in cisplatin-induced nephrotoxicity in rats. *Pak. Vet. J*., **42**(3): 376-382.

Wu E (2021). Curcumin-loaded lipid and polymer nanoparticles for Alzheimer's disease treatment. *Int. J. Biomed. Sci.*, **17**(3): 34-39.

Zhang Y, Jiao L, Wu Z, Gu P, Feng Z, Xu S, Liu Z, Yang Y and Wang D (2022). Fabrication and characterization of Chinese yam polysaccharides PLGA nanoparticles stabilized Pickering emulsion as an efficient adjuvant. *Int. J. Biol. Macromol*., **209**(1): 513-524.

Zhong Q, Sun Y, Xu Y, Khan A, Guo J, Wang Z, Sun N and Li H (2021). The therapeutic effect and mechanism of physalin on LPS-induced acute lung injury in rats. *Pak. Vet. J*., **41**(3): 372-378.